

Observation and Measurements of Vector-Boson Pair Production with ATLAS

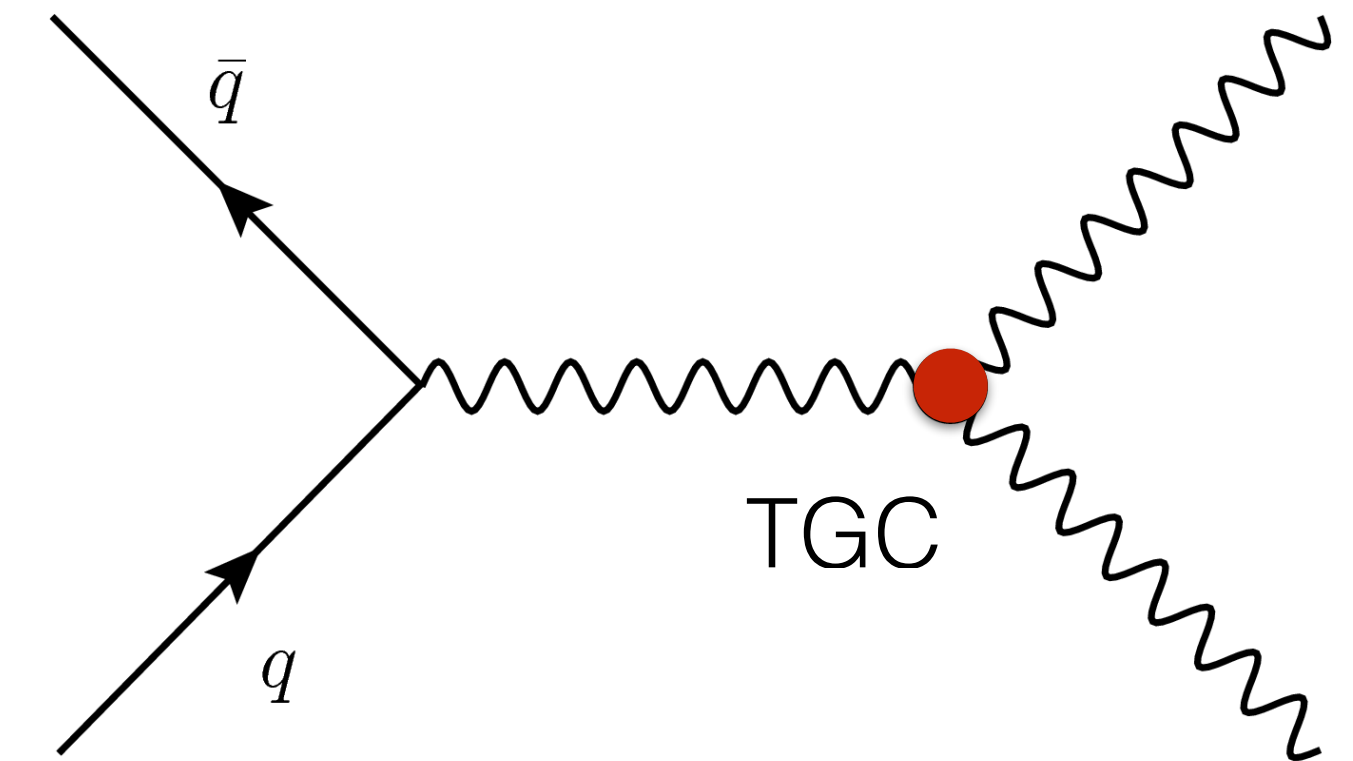
Rebecca Linck

On Behalf of the ATLAS Collaboration

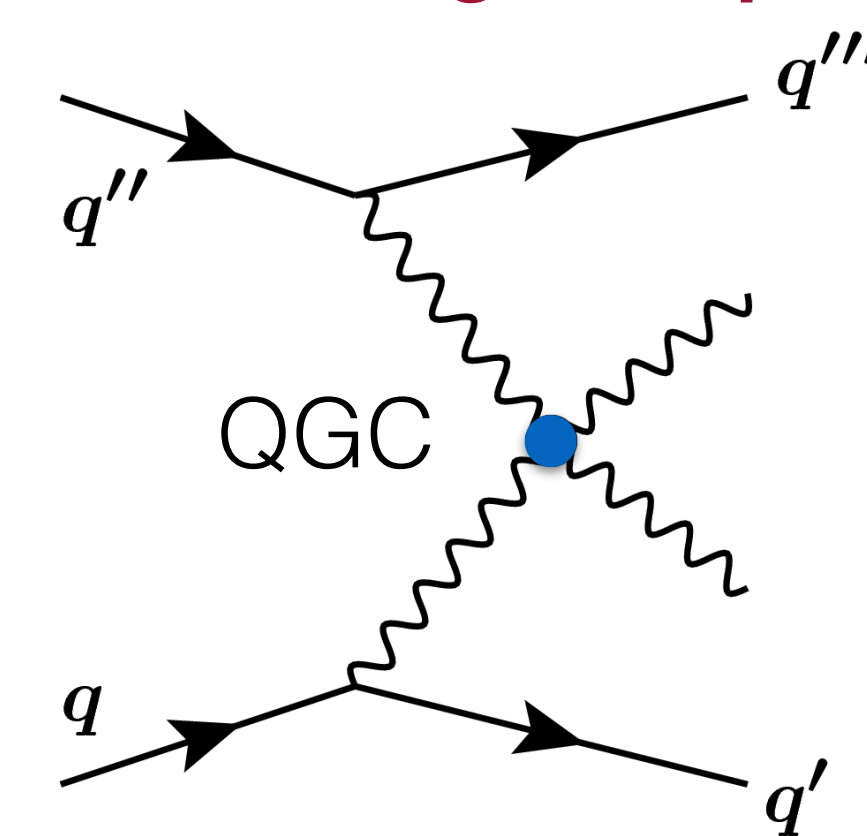
ALPS 2019
22-27 April 2019

- The ATLAS detector has recently been used to study a number of electroweak vector-boson pair production processes.
- Among these processes are the invisible Z, VBS and inclusive $W^\pm Z$, inclusive W^+W^- and VBS $W^\pm W^\pm$.
- Using these vector-boson pair production processes we can,
 - Probe the electroweak sector of the Standard Model.
 - Investigate the mechanism responsible for electroweak symmetry breaking.
 - Study triple and quartic gauge-boson interactions.
 - Search for evidence of new physics (BSM, aTGC, aQGC, etc.)

Triple Gauge Coupling



Quartic Gauge Coupling



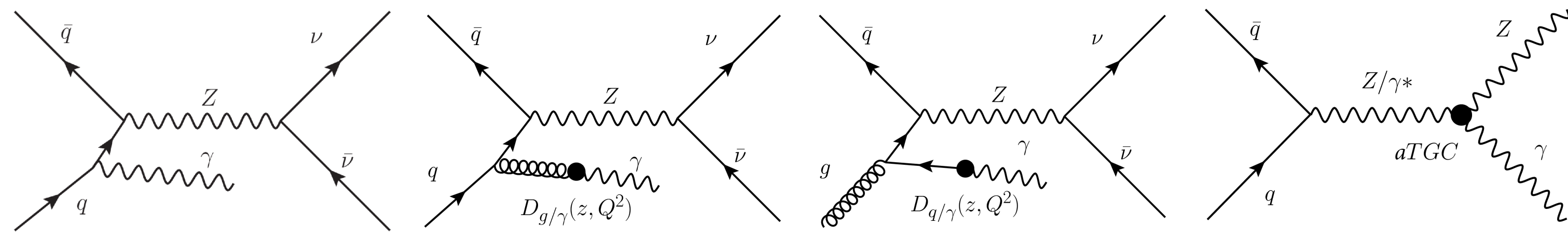
- Data conditions for all of the included measurements:
 - High energy proton-proton collisions recorded in 2015-2016 at $\sqrt{s} = 13$ TeV and $\mathcal{L} = 36.1$ fb $^{-1}$.

$Z\gamma \rightarrow \nu\bar{\nu}\gamma$

Z Boson Production in Association with a High Energy Photon

[arXiv:1810.04995](https://arxiv.org/abs/1810.04995)

- $Z\gamma \rightarrow \nu\bar{\nu}\gamma$ events with exactly one tight isolated photon and no leptons.
- Events are selected in an inclusive region ($N_{\text{jets}} \geq 0$) and an exclusive region ($N_{\text{jets}} = 0$).

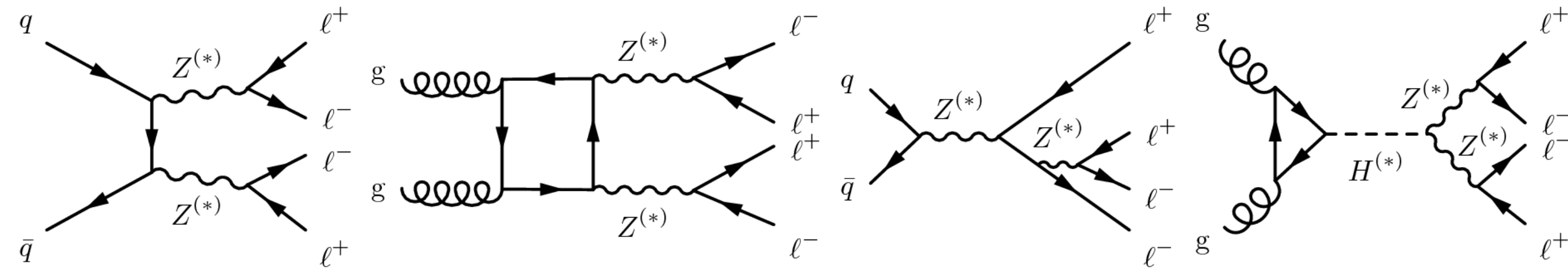


$pp \rightarrow 4\ell$

Four-lepton ($pp \rightarrow 4\ell$) Production

[arXiv:1902.05892](https://arxiv.org/abs/1902.05892)

- A set of processes with four leptons in the final state ($pp \rightarrow 4\ell$).
- $4\ell = 4e, 4\mu$ or $2e2\mu$.



Inc. $W^\pm Z$

Inclusive $W^\pm Z$ Production

[arXiv:1902.05759](https://arxiv.org/abs/1902.05759)

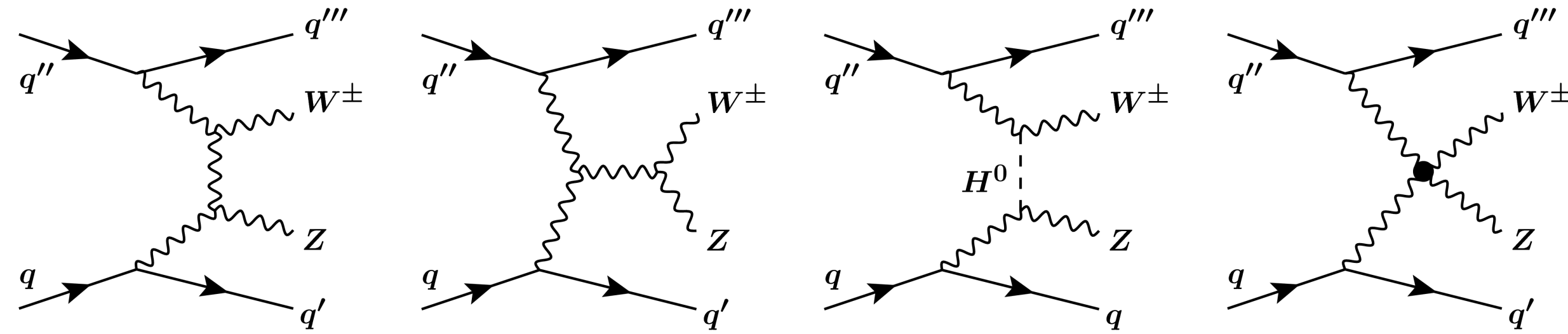
- $W^\pm Z$ production characterized by a decay to three leptons and a neutrino.
- $W^\pm \rightarrow \ell^\pm \nu$ ($\ell = e$ or μ) and $Z \rightarrow \ell\ell$ ($\ell\ell = e^+e^-$ or $\mu^+\mu^-$)
- Events include any number of jets.

VBS $W^\pm Z$

Electroweak VBS $W^\pm Zjj$ Production

[arXiv:1812.09740](https://arxiv.org/abs/1812.09740)

- The purely electroweak scattering of two vector bosons yielding a W^\pm boson, a Z boson and two jets ($W^\pm Zjj$ -EW).
- The W^\pm and Z bosons decay into three leptons and a neutrino. $W^\pm \rightarrow \ell^\pm \nu$ and $Z \rightarrow \ell\ell$, ($\ell = e$ and/or μ).



Inc. W^+W^-

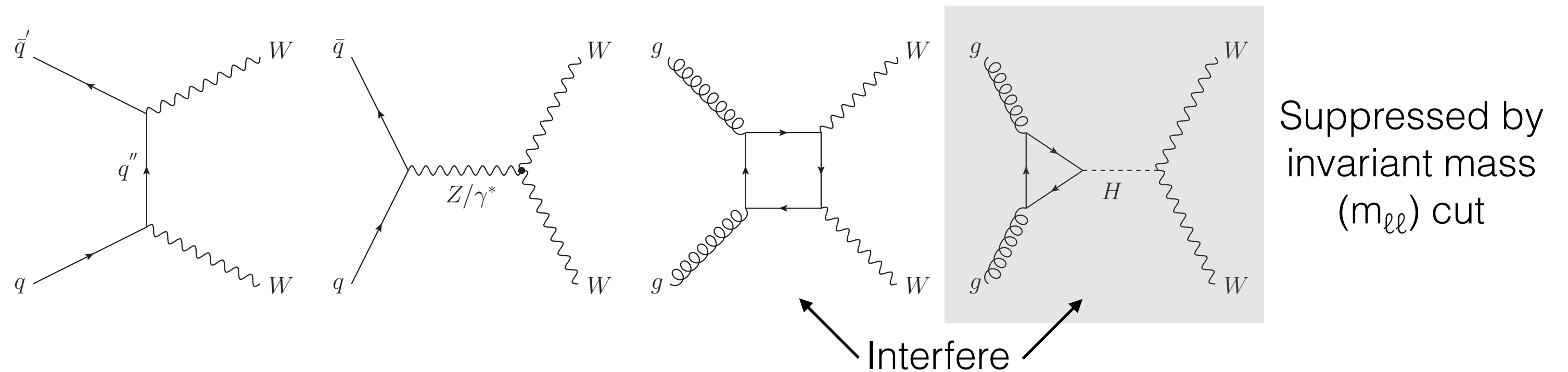
Inclusive Opposite-Sign W Boson Pair Production

[ATL-COM-PHYS-2018-1487](https://atlas.cern/ATL-COM-PHYS-2018-1487)

- W^+W^- production characterized by a decay to two leptons, two neutrinos and no jets.

$$W^+W^- \rightarrow e^\pm \nu \mu^\mp \bar{\nu}$$

- This analysis is orthogonal to the recent $H \rightarrow WW^*$ analysis.



VBS $W^\pm W^\pm$

VBS Same-Sign W Boson Pair Production

[ATLAS-CONF-2018-030](https://atlas.cern/ATLAS-CONF-2018-030)

- The electroweak scattering of two vector bosons yielding two same-sign W bosons and two jets.
- Each W boson decays into a lepton and a neutrino. $W^\pm \rightarrow \ell^\pm \nu$, ($\ell = e$ and/or μ).

- In invisible Z boson ($Z\gamma \rightarrow \nu\bar{\nu}\gamma$) analysis, both the fiducial and differential cross-sections are measured in an extended fiducial region where many of the analysis cuts have been relaxed, (including the lepton veto).

The Fiducial Cross-Section:

- The measured fiducial cross-sections are listed in the table to the right.
- The measured fiducial cross-sections agree within one standard deviation with the SM prediction.

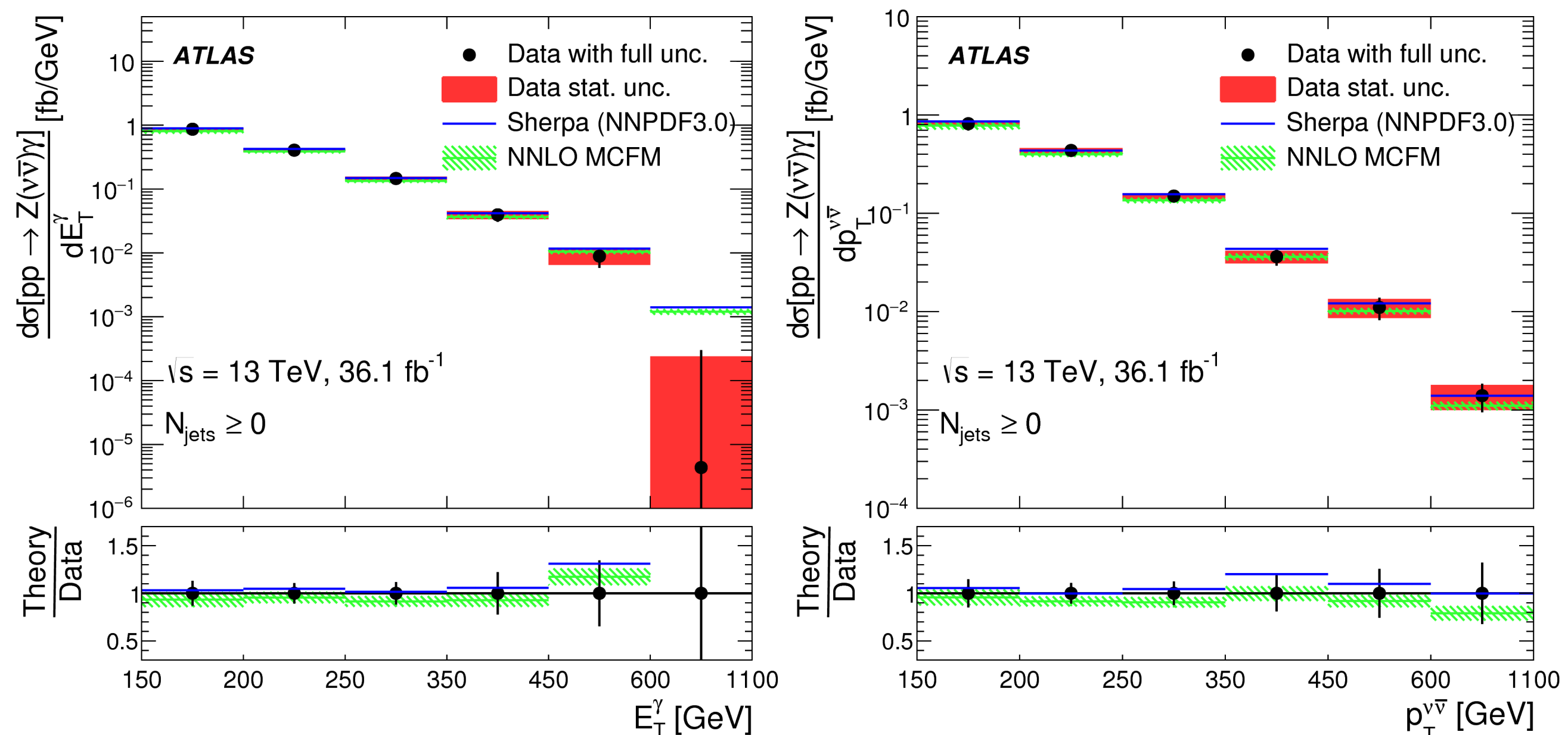
The Differential Cross-Section:

- The differential cross-sections are extracted using an iterative Bayesian unfolding method.
- The measured differential cross-sections generally show good agreement with the SM prediction.
- The disagreement in the last bin of the E_T^γ distribution is due to statistical fluctuation.

Fiducial Cross-Sections

$\sigma^{\text{ext.fid.}}$ [fb] Measurement	$\sigma^{\text{ext.fid.}}$ [fb] NNLO MCFM Prediction
$N_{\text{jets}} \geq 0$	
$83.7^{+3.6}_{-3.5}$ (stat.) $^{+6.9}_{-6.2}$ (syst.) $^{+1.7}_{-2.0}$ (lumi.)	78.1 ± 0.2 (stat.) ± 4.7 (syst.)
$N_{\text{jets}} = 0$	
$52.4^{+2.4}_{-2.3}$ (stat.) $^{+4.0}_{-3.6}$ (syst.) $^{+1.2}_{-1.1}$ (lumi.)	55.9 ± 0.1 (stat.) ± 3.9 (syst.)

Inclusive Differential Cross-Sections



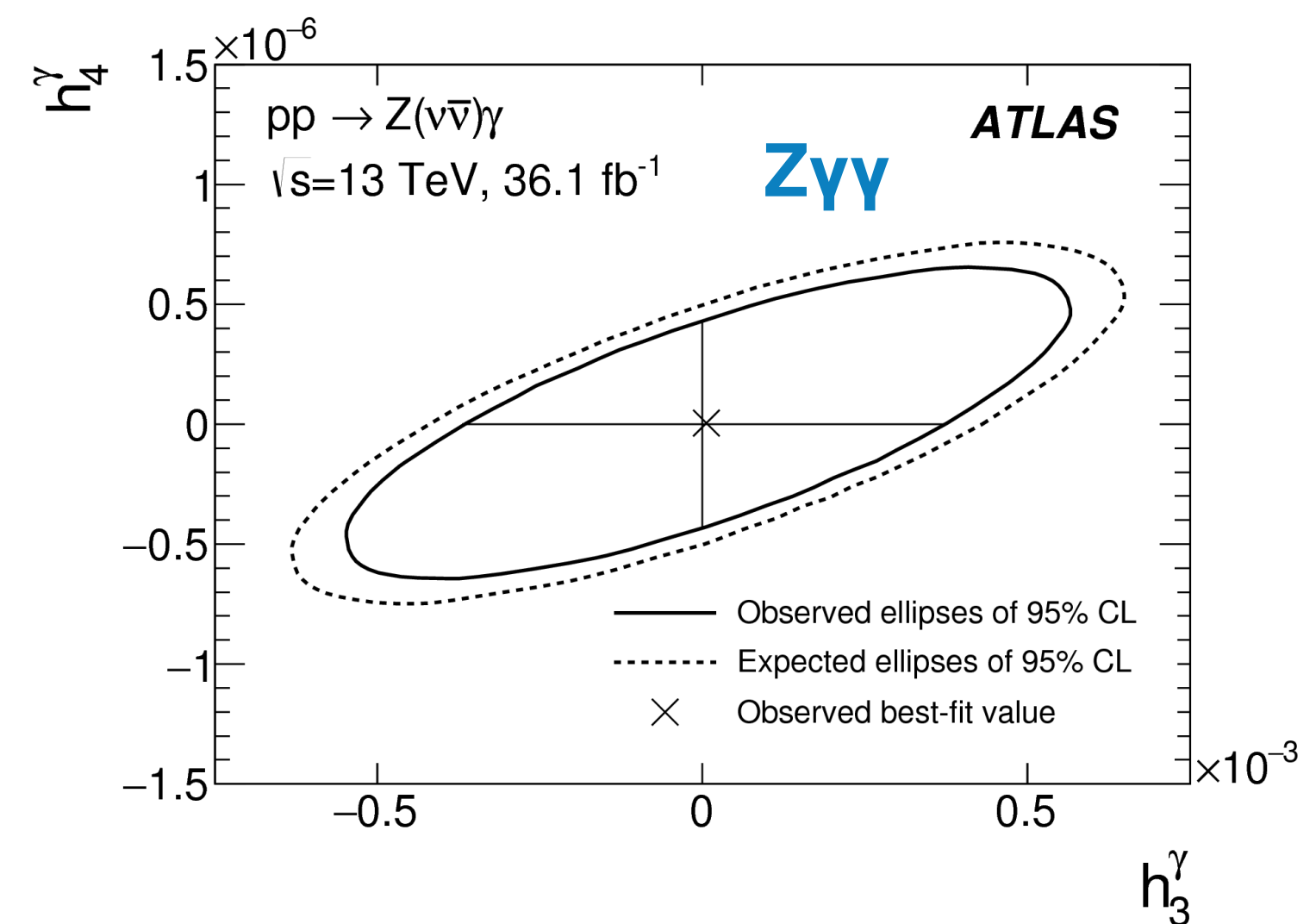
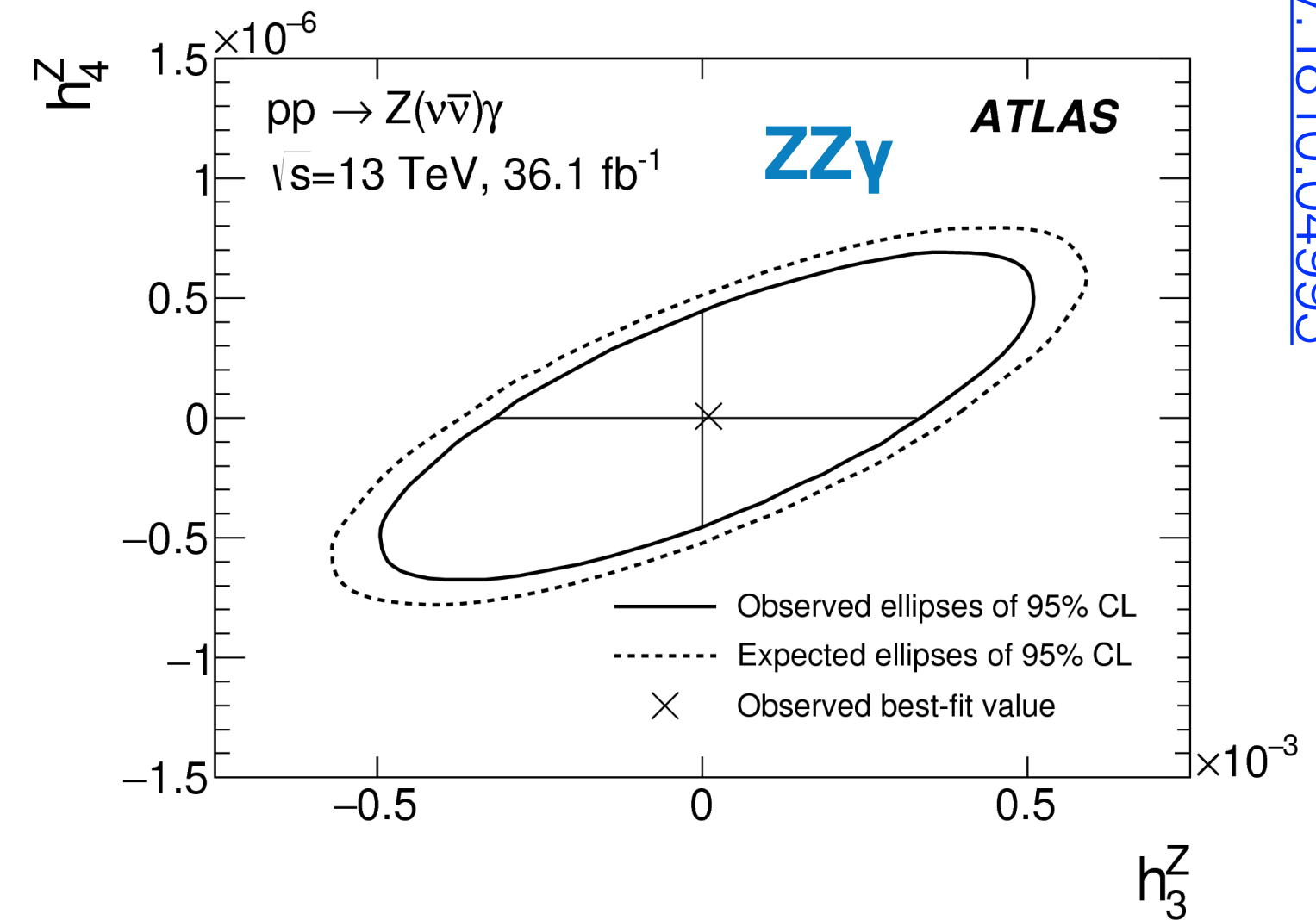
- In the framework of the effective vertex function approach, this analysis parameterizes aTGC contributions as follows.
 - CP-violating: h_1^V and h_2^V
 - CP-conserving: h_3^V and h_4^V
- $$\left. \begin{array}{l} \text{CP-violating: } h_1^V \text{ and } h_2^V \\ \text{CP-conserving: } h_3^V \text{ and } h_4^V \end{array} \right\} V = Z \text{ or } \gamma, \text{ where, } \begin{cases} Z = ZZ\gamma \text{ vertex} \\ \gamma = Z\gamma\gamma \text{ vertex} \end{cases}$$
- The CP-violating and the CP-conserving parameters do not interfere and are nearly identical.
 - To optimize the sensitivity to aTGCs, the exclusive region ($N_{\text{jets}} = 0$) is used with the additional requirement that $E_T^\gamma > 600$ GeV.

- Shown here are the 1D 95% confidence level limits for the CP-conserving parameters.

Parameter	Limit 95% CL	
	Measured	Expected
h_3^γ	$(-3.7 \times 10^{-4}, 3.7 \times 10^{-4})$	$(-4.2 \times 10^{-4}, 4.3 \times 10^{-4})$
h_3^Z	$(-3.2 \times 10^{-4}, 3.3 \times 10^{-4})$	$(-3.8 \times 10^{-4}, 3.8 \times 10^{-4})$
h_4^γ	$(-4.4 \times 10^{-7}, 4.3 \times 10^{-7})$	$(-5.1 \times 10^{-7}, 5.0 \times 10^{-7})$
h_4^Z	$(-4.5 \times 10^{-7}, 4.4 \times 10^{-7})$	$(-5.3 \times 10^{-7}, 5.1 \times 10^{-7})$

- This analysis did not observe anomalous couplings.
- When compared with previous analyses, this analysis imposes 3-7 times more stringent limits on anomalous couplings.

95% CL Ellipses



arXiv:1810.04995

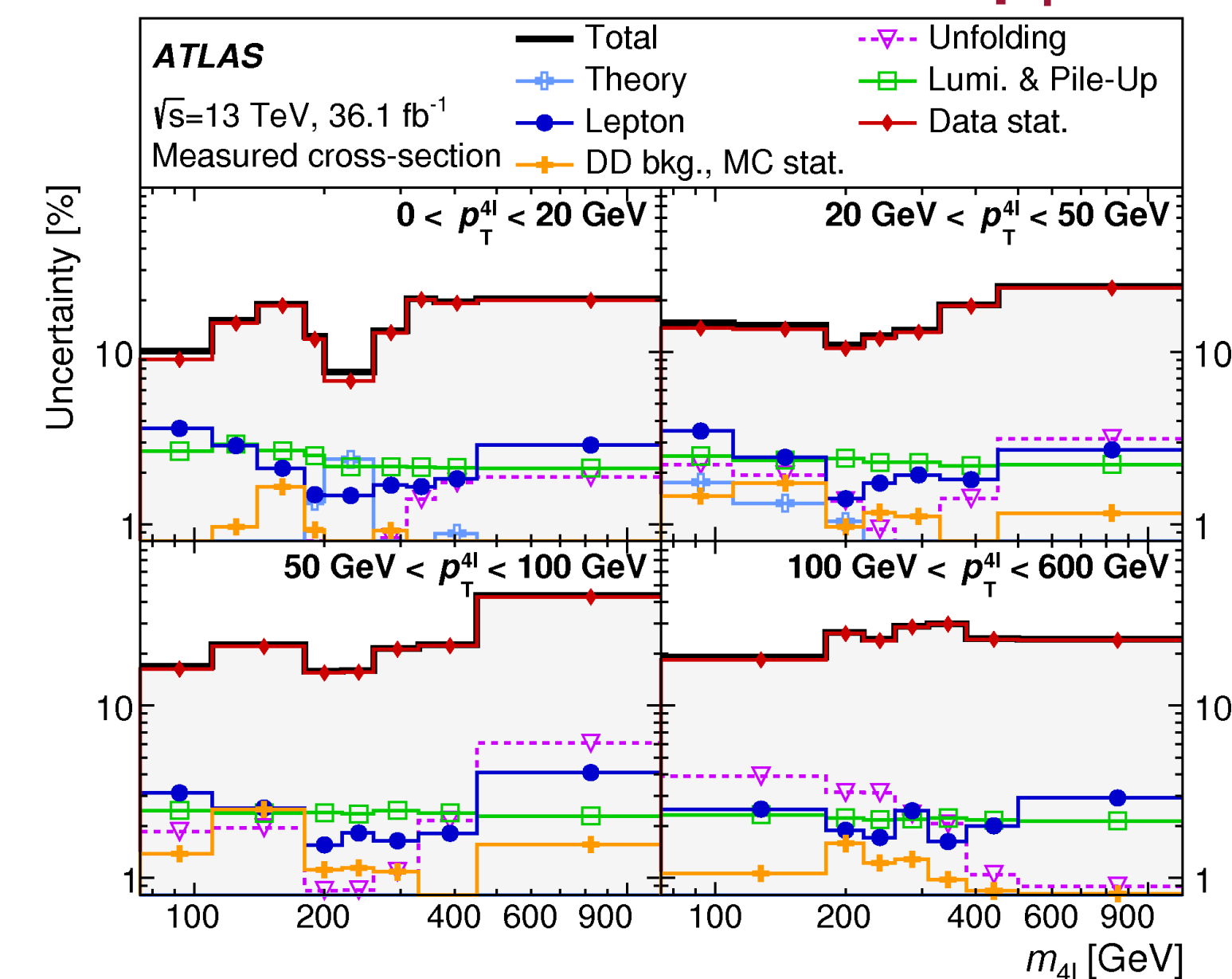
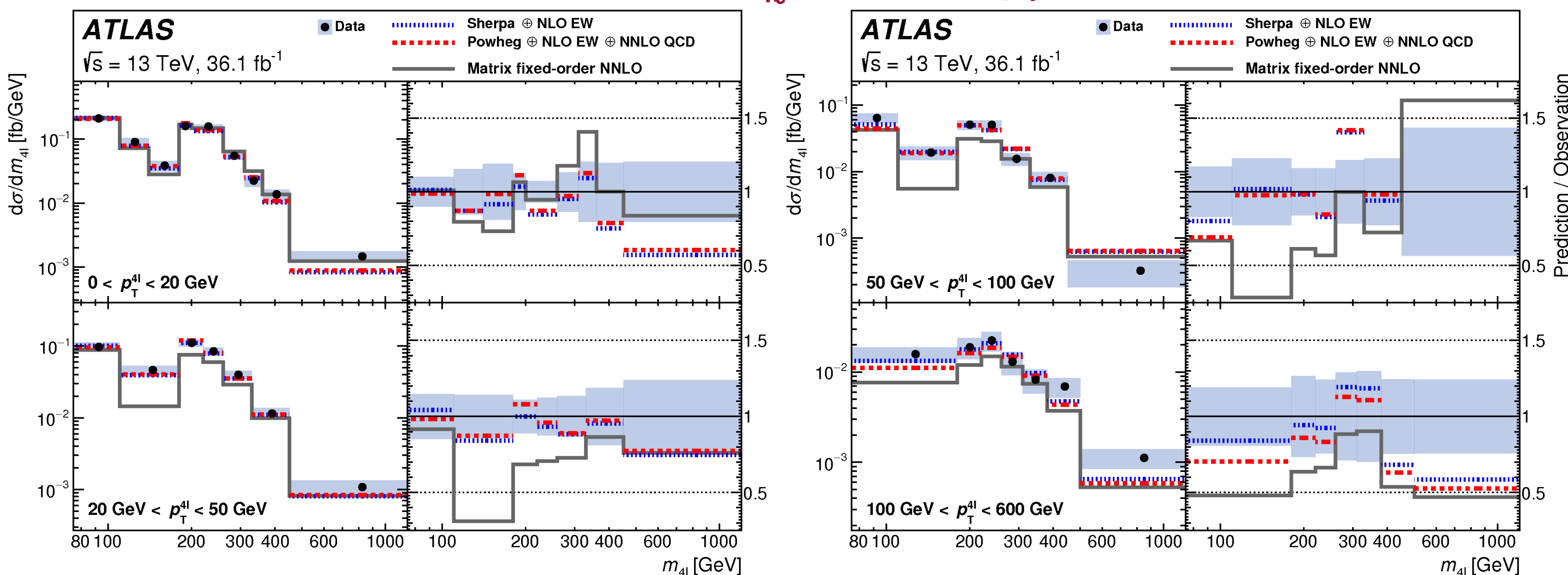
Differential Cross-Section:

- In the four lepton ($pp \rightarrow 4\ell$) analysis, the differential cross-section is determined as a function of the invariant mass, $m_{4\ell}$.
- Overall, good agreement exists between the unfolded data and the predictions found using Sherpa and Powheg.
- The MATRIX prediction shows the effect of additional higher-order corrections and QED final state radiation.
- As can be seen to the right below, the overall cross-section uncertainty is dominated by the statistical uncertainty.

arXiv:1902.05892

Measured Differential Cross-Section as a Function of $m_{4\ell}$, in Bins of $p_T^{4\ell}$

Leading Sources of Uncertainty in Cross-Section in Bins of $p_T^{4\ell}$



Signal strength for gluon-induced 4ℓ production ($gg \rightarrow 4\ell$).

- Is determined relative to an uncorrected leading-order precision MCFM prediction.

$$\mu_{gg}^{LO} = \frac{\sigma_{gg \rightarrow 4\ell}^{\text{measured}}}{\sigma_{gg \rightarrow 4\ell}^{\text{SM, LO QCD}}}$$

	ATLAS at $\sqrt{s} = 13$ TeV	ATLAS at $\sqrt{s} = 8$ TeV
Measured	2.7 ± 0.9	2.4 ± 1.4
Expected	2.2 ± 0.9	

Branching Fraction of $Z \rightarrow 4\ell$

- Is determined in a region that is dominated by single Z boson production.

$$80 < m_{4\ell} < 100 \text{ GeV and } m_{\ell\ell} > 4 \text{ GeV}$$

Measurement	$\mathcal{B}_{Z \rightarrow 4\ell} / 10^{-6}$
ATLAS, $\sqrt{s} = 7$ TeV and 8 TeV [8]	$4.31 \pm 0.34(\text{stat}) \pm 0.17(\text{syst})$
CMS, $\sqrt{s} = 13$ TeV [6]	$4.83^{+0.23}_{-0.22}(\text{stat})^{+0.32}_{-0.29}(\text{syst}) \pm 0.08(\text{theo}) \pm 0.12(\text{lumi})$
ATLAS, $\sqrt{s} = 13$ TeV	$4.70 \pm 0.32(\text{stat}) \pm 0.21(\text{syst}) \pm 0.14(\text{lumi})$

Constraint on Off-Shell Higgs Boson Signal Strength

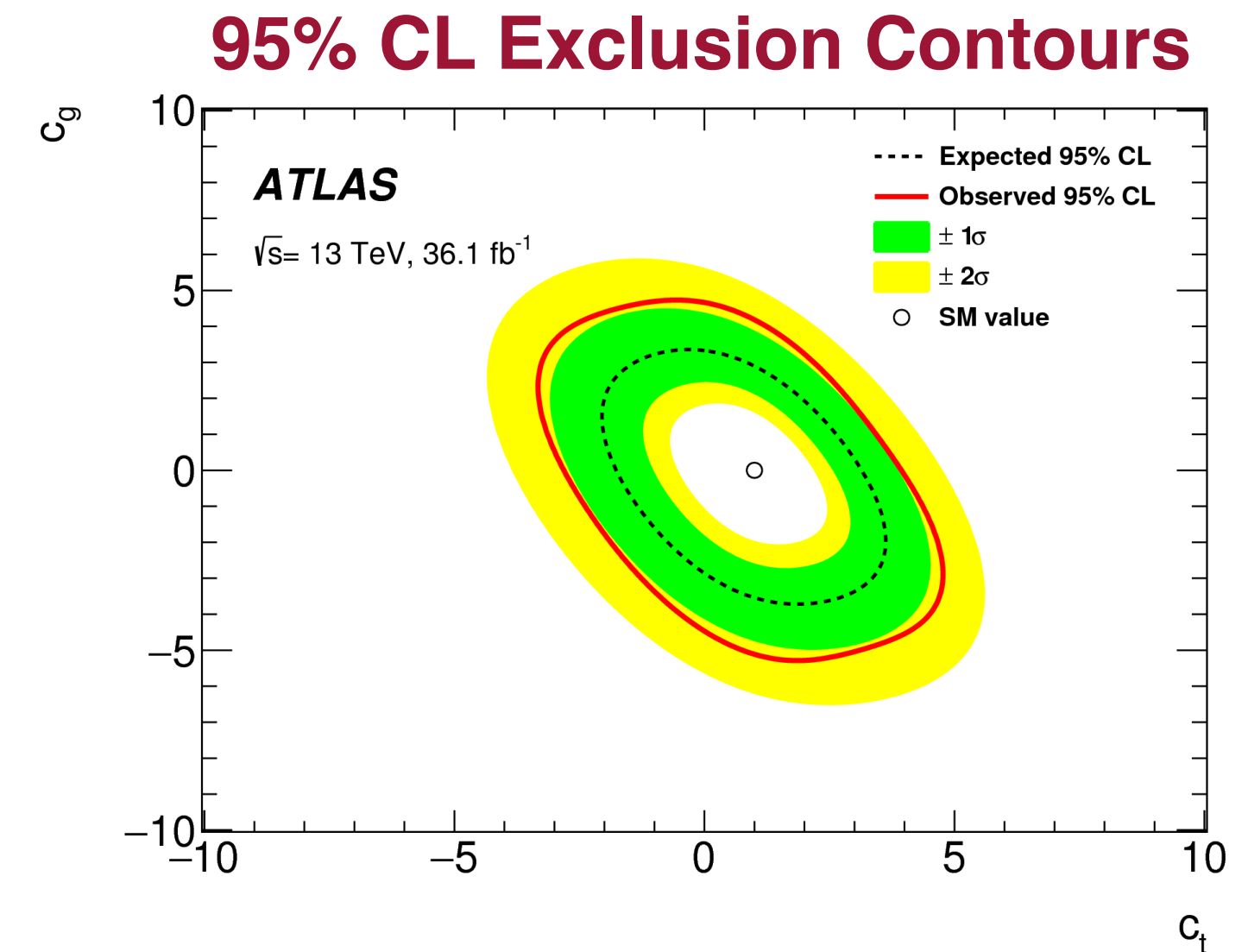
- Is determined using the double-differential distribution for $m_{4\ell}$ in terms of D_{ME} (matrix-element discriminant) at high mass ($m_{4\ell} > 180$ GeV).

	95% CL Upper Limit for Off-Shell Higgs Boson Signal Strength
Observed	6.5
Expected	5.4

- The observed value of the 95% CL upper limit agrees with the expected within $\pm 1\sigma$ uncertainty.

Constraint on Modified Higgs Boson Couplings

- Is determined at high mass (> 180 GeV) for two BSM couplings.
- c_t ($t\bar{t}H$) and c_g (ggH)
- The parameter space outside of the observed contour is excluded at 95% CL.

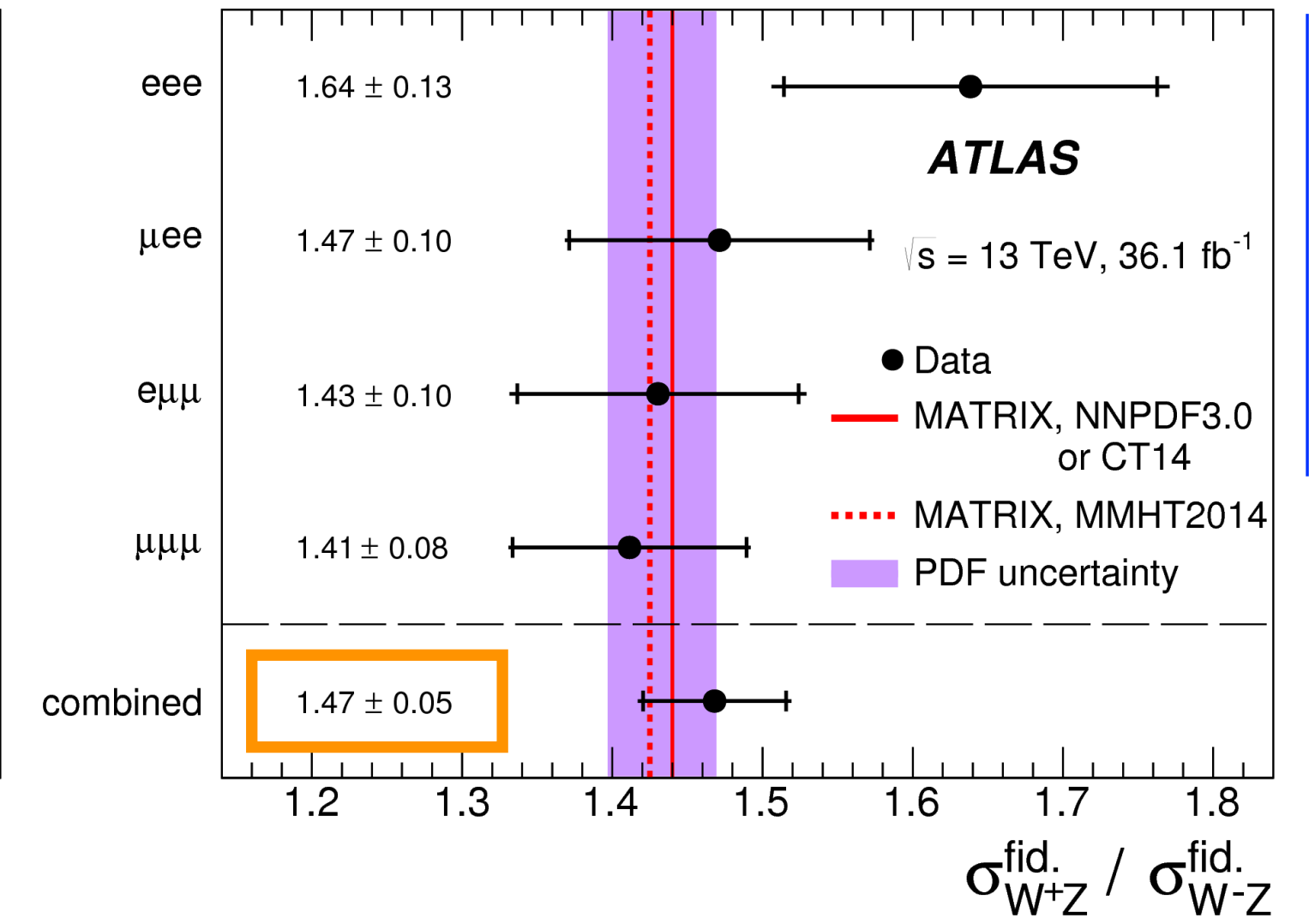
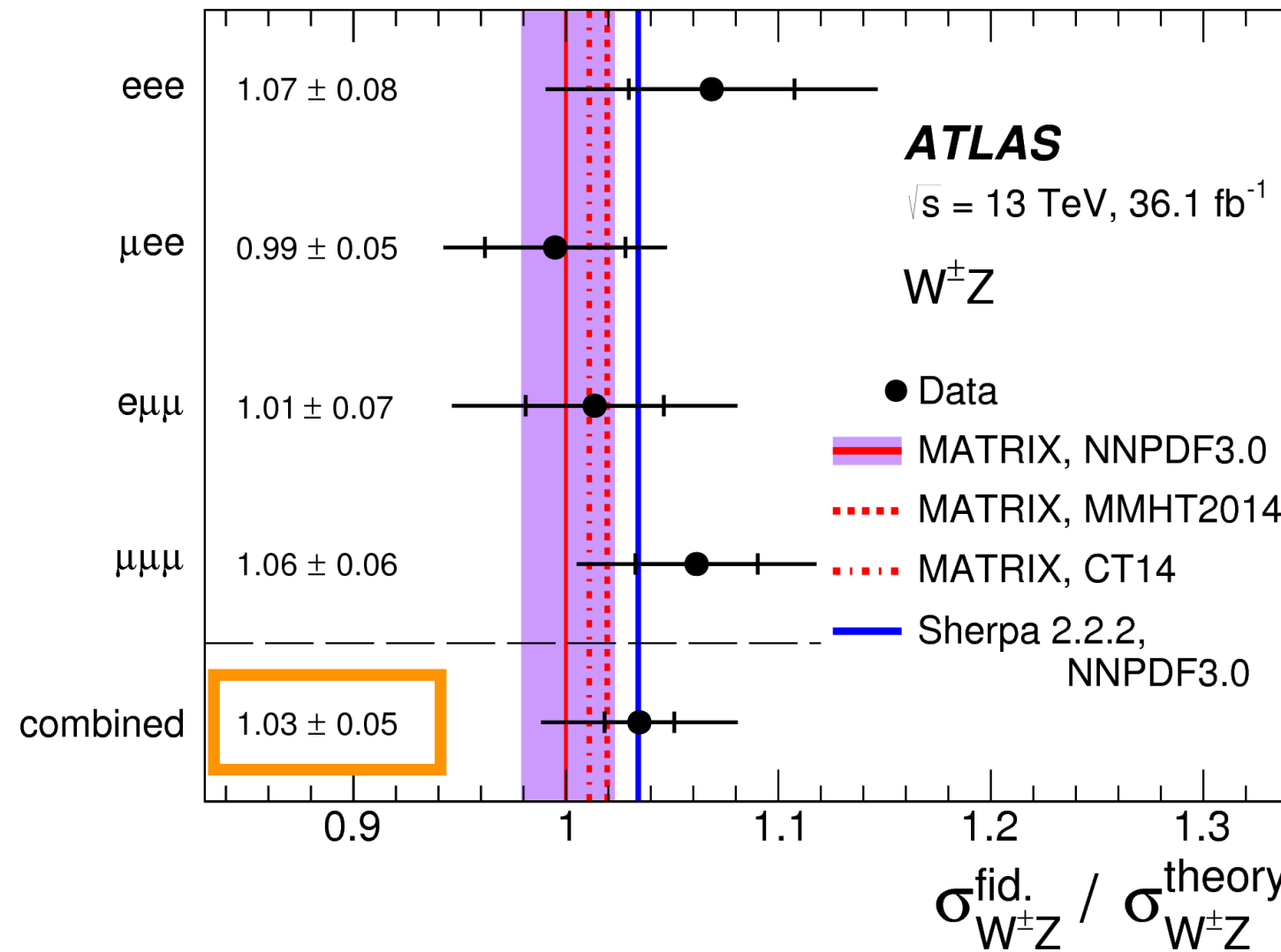


The Fiducial Cross-Section:

- In the inclusive $W^{\pm}Z$ analysis, the fiducial cross section is determined separately in the different lepton channels for W^-Z , W^+Z and $W^{\pm}Z$.

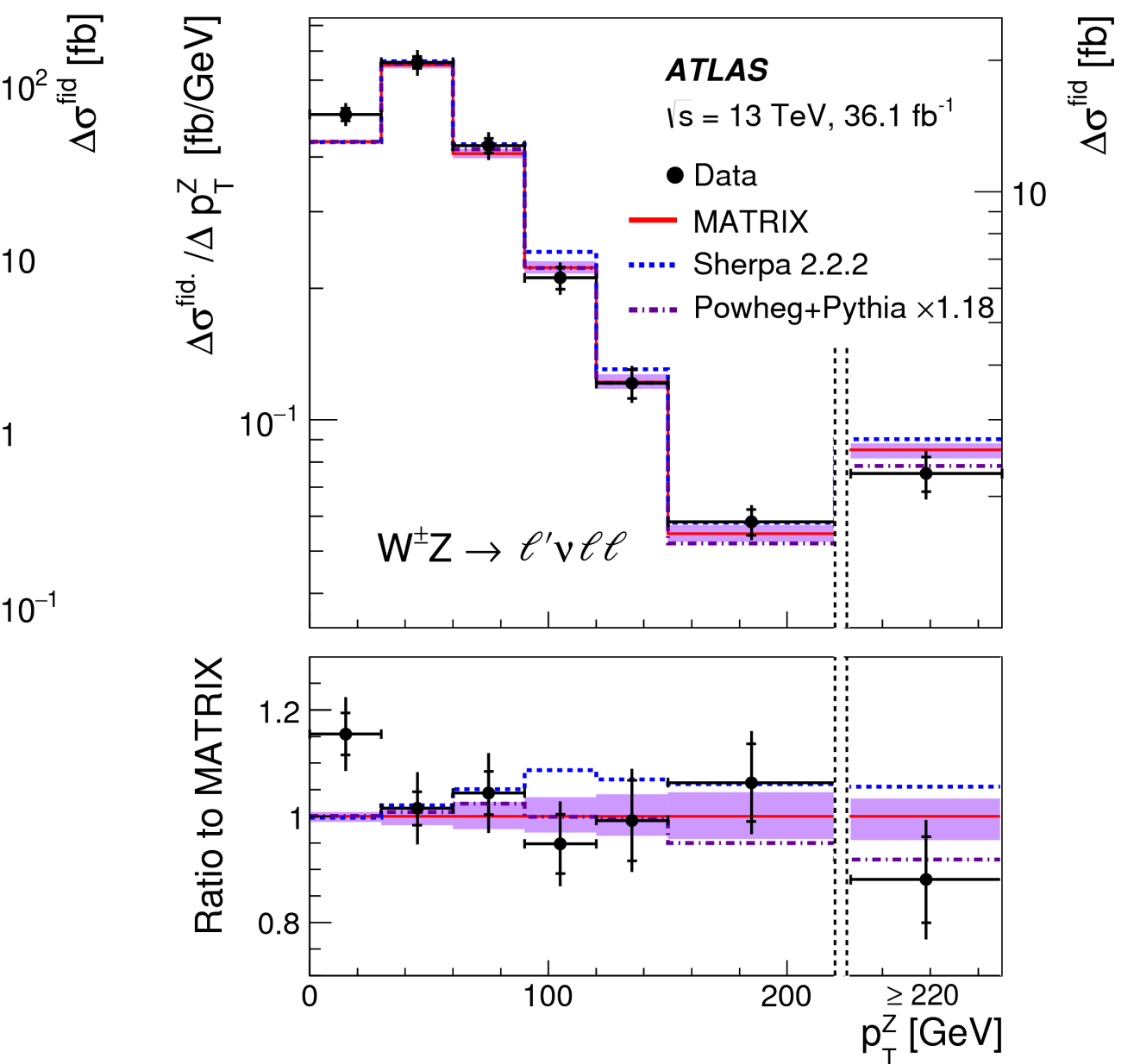
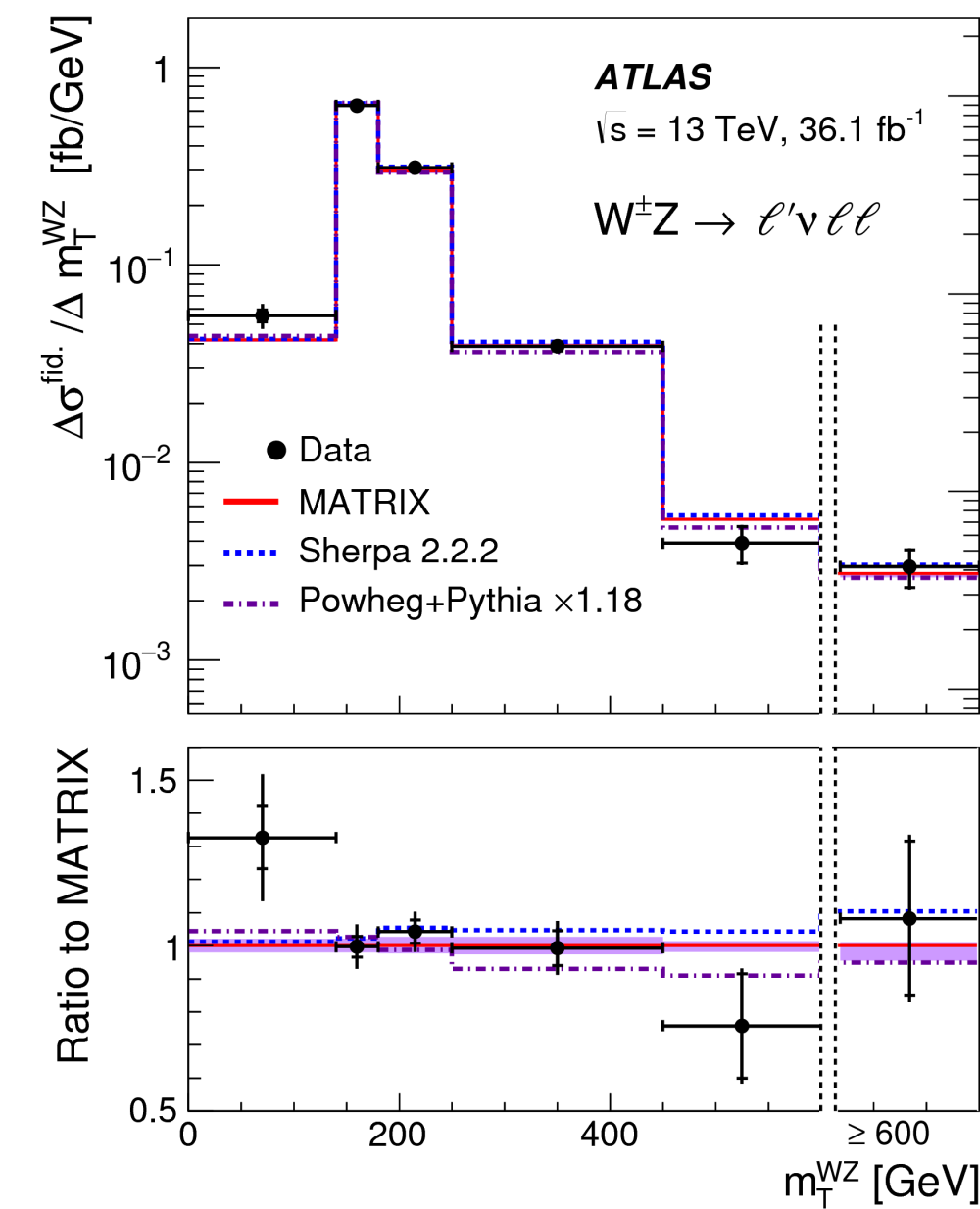
$$\sigma_{W^{\pm}Z \rightarrow \ell'\nu\ell\ell}^{\text{fid.}} = \frac{N_{\text{data}} - N_{\text{bkg}}}{\mathcal{L} \cdot C_{WZ}} \times \left(1 - \frac{N_{\tau}}{N_{\text{all}}}\right)$$

- A χ^2 minimization method is used to combine the results from the four lepton channels.



The Differential Cross-Section:

- The differential cross-section is determined for a combination of all four lepton channels as a function of several variables.
- Good agreement exists between the unfolded data and the prediction for each of the resulting distributions.
- The high energy tails of the m_T^{WZ} and p_T^Z distributions are sensitive to aTGC.
- As shown here, there is no excess of data events in the associated bins and thus no evidence of aTGC.



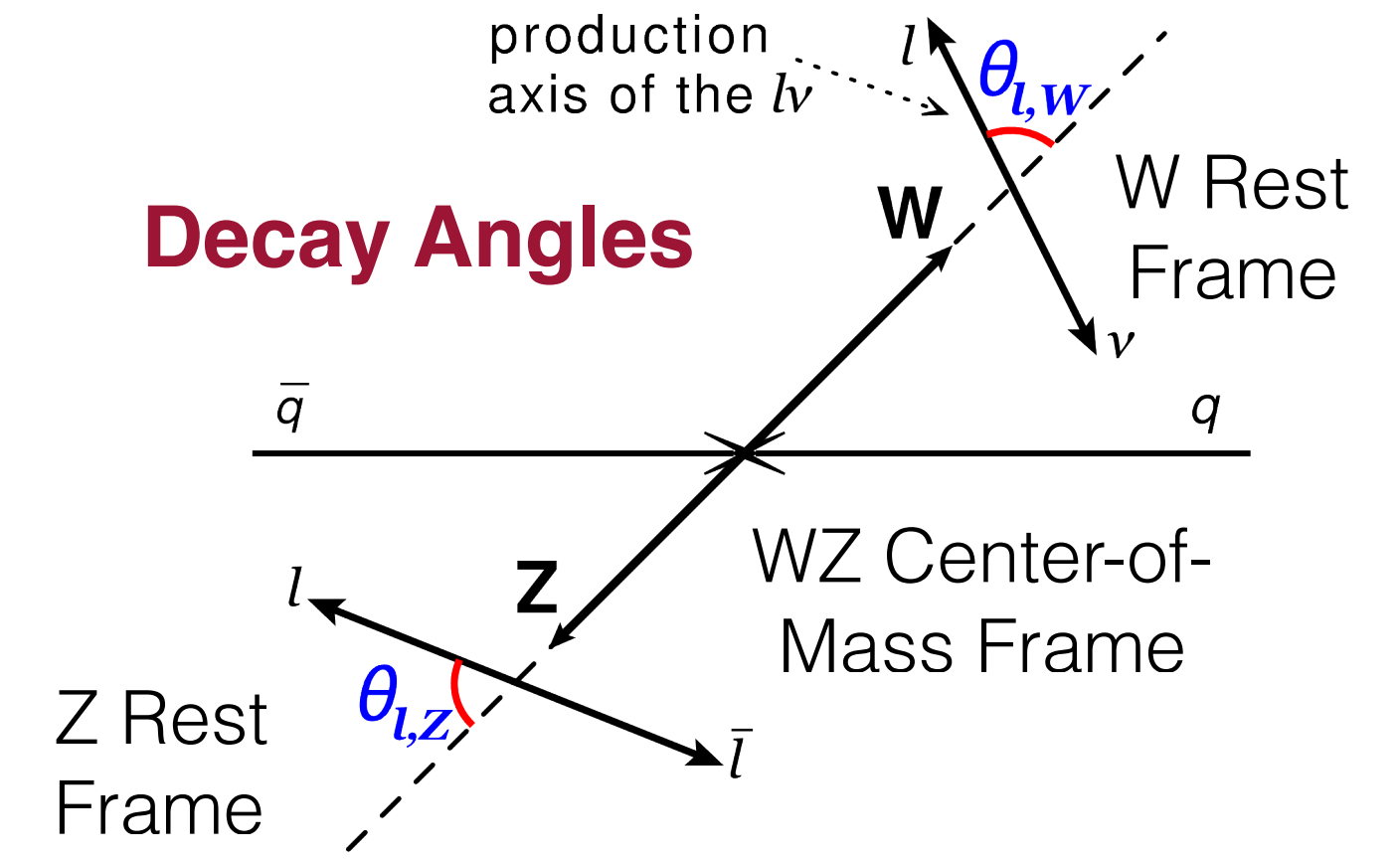
arXiv:1902.05759

Polarization of WZ Events:

- The W and Z boson polarization measurements are performed on a sum of the four lepton channels (eee, eμμ, μee, and μμμ).
- Binned profile-likelihood fits are performed of templates of the helicity states.
- The helicity parameters, f_0 and $f_L - f_R$, are extracted from fits of $q_\ell \cdot \cos(\theta_{\ell,W})$ and $\cos(\theta_{\ell,Z})$ for W and Z separately.
- The resulting significance of the longitudinal helicity fractions, f_0 :

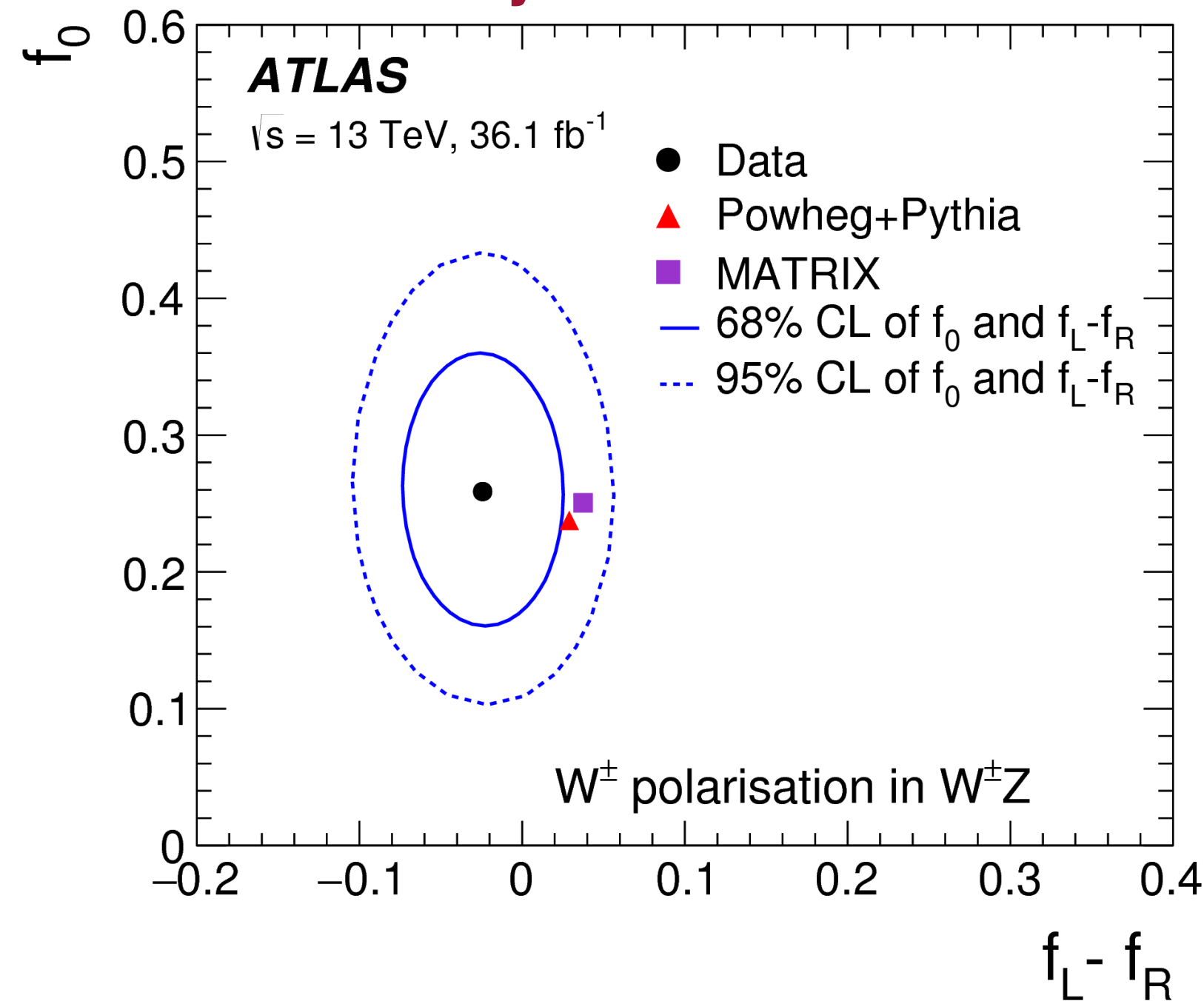
	Significance	
	Observed	Predicted
W^\pm	4.2σ	3.8σ
Z	6.5σ	6.1σ

- Note that the f_0 for the W is more difficult to extract and thus has greater uncertainty.
- This analysis successfully observed longitudinally polarized W bosons.

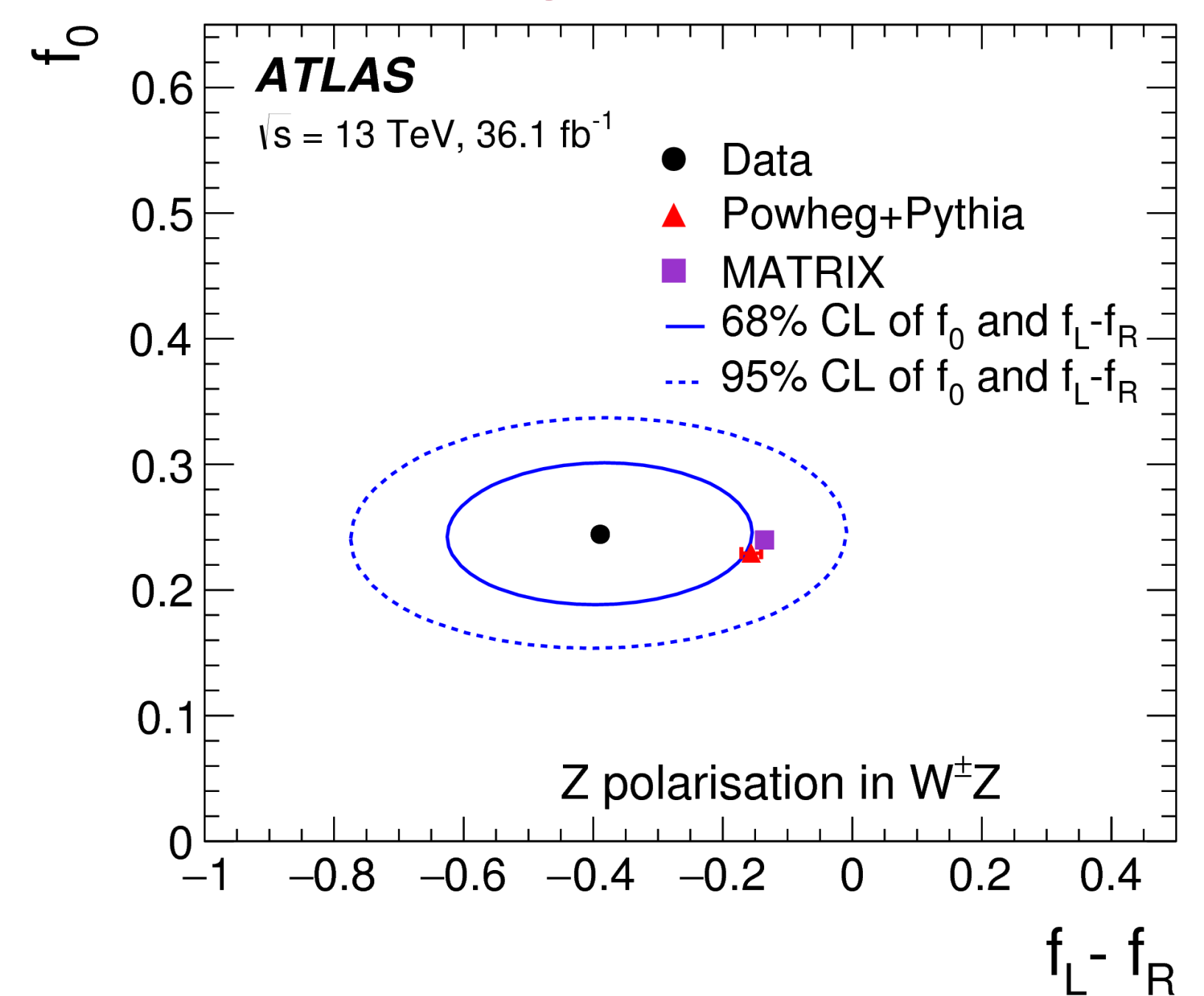


arXiv:1902.05759

Helicity Fractions for W^\pm



Helicity Fractions for Z



Fiducial Cross-Section:

- In the electroweak VBS W $^{\pm}$ Zjj analysis, two fiducial cross-sections are determined.

- The BDT score is used to extract the signal significance ($\mu_{WZjj-EW}$). The fiducial cross-section for W $^{\pm}$ Zjj-EW production is then derived from $\mu_{WZjj-EW}$.

$$\mu_{WZjj-EW} = \frac{N_{\text{data}}^{\text{signal}}}{N_{\text{MC}}^{\text{signal}}} = \frac{\sigma_{WZjj-EW}^{\text{fid.}}}{\sigma_{WZjj-EW}^{\text{fid.,MC}}}$$

- Signal Significance: $\mu_{WZjj-EW} = 1.77^{+0.44}_{-0.40}$ (stat.) $^{+0.15}_{-0.12}$ (exp. syst.) $^{+0.15}_{-0.12}$ (mod. syst.) $^{+0.04}_{-0.02}$ (lumi.) = $1.77^{+0.49}_{-0.43}$

- Measured cross-section: $\sigma_{WZjj-EW}^{\text{fid.}} = 0.57^{+0.14}_{-0.13}$ (stat.) $^{+0.05}_{-0.04}$ (exp. syst.) $^{+0.05}_{-0.04}$ (mod. syst.) $^{+0.01}_{-0.01}$ (lumi.) fb = $0.57^{+0.16}_{-0.14}$ fb

- Predicted cross-section: $\sigma_{WZjj-EW}^{\text{fid., Sherpa}} = 0.321 \pm 0.002$ (stat.) ± 0.005 (PDF) $^{+0.027}_{-0.023}$ (scale) fb

- The integrated fiducial cross-section for all W $^{\pm}$ Zjj production (W $^{\pm}$ Zjj-EW and W $^{\pm}$ Zjj-QCD) can be expressed as,

$$\sigma_{W^{\pm}Zjj}^{\text{fid.}} = \frac{N_{\text{data}} - N_{\text{bkg}}}{\mathcal{L} \cdot C_{WZjj}} \times \left(1 - \frac{N_{\tau}}{N_{\text{all}}} \right)$$

- Measured cross-section: $\sigma_{W^{\pm}Zjj}^{\text{fid.}} = 1.68 \pm 0.16$ (stat.) ± 0.12 (exp. syst.) ± 0.13 (mod. syst.) ± 0.044 (lumi.) fb = 1.68 ± 0.25 fb

- Predicted cross-section: $\sigma_{W^{\pm}Zjj}^{\text{fid., Sherpa}} = 2.15 \pm 0.01$ (stat.) ± 0.05 (PDF) $^{+0.65}_{-0.44}$ (scale) fb

- Both measured fiducial cross-sections include interference effects between W $^{\pm}$ Zjj-QCD and W $^{\pm}$ Zjj-EW.
- Neither of the predicted fiducial cross-sections include interference effects between W $^{\pm}$ Zjj-QCD and W $^{\pm}$ Zjj-EW. They are also determined at LO and do not include NLO Electroweak corrections.

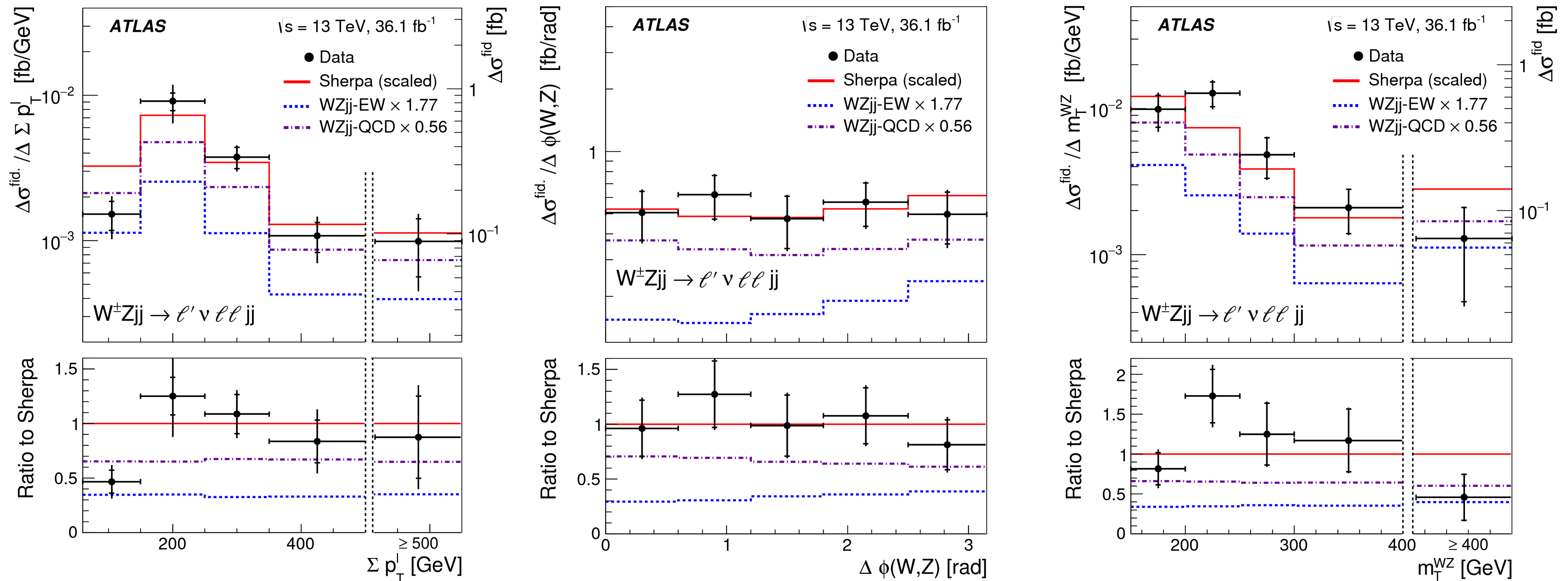
Differential Cross-Section:

- An iterative Bayesian unfolding is performed to measure the $W^\pm Zjj$ differential cross-section.
- Shown here is the differential cross-section as a function of three variables that are sensitive to aQGCs.

- The $WZjj$ -EW and $WZjj$ -QCD predicted cross-sections have been scaled by their respective signal strengths to more closely model data and minimize unfolding uncertainties.

- Sherpa samples for $WZjj$ -EW and $WZjj$ -QCD have also been added together and similarly scaled.

Differential Cross-Section as a Function of Σp_T^ℓ , $\Delta\phi(W,Z)$ and m_T^{WZ}



- For the inclusive W^+W^- analysis:

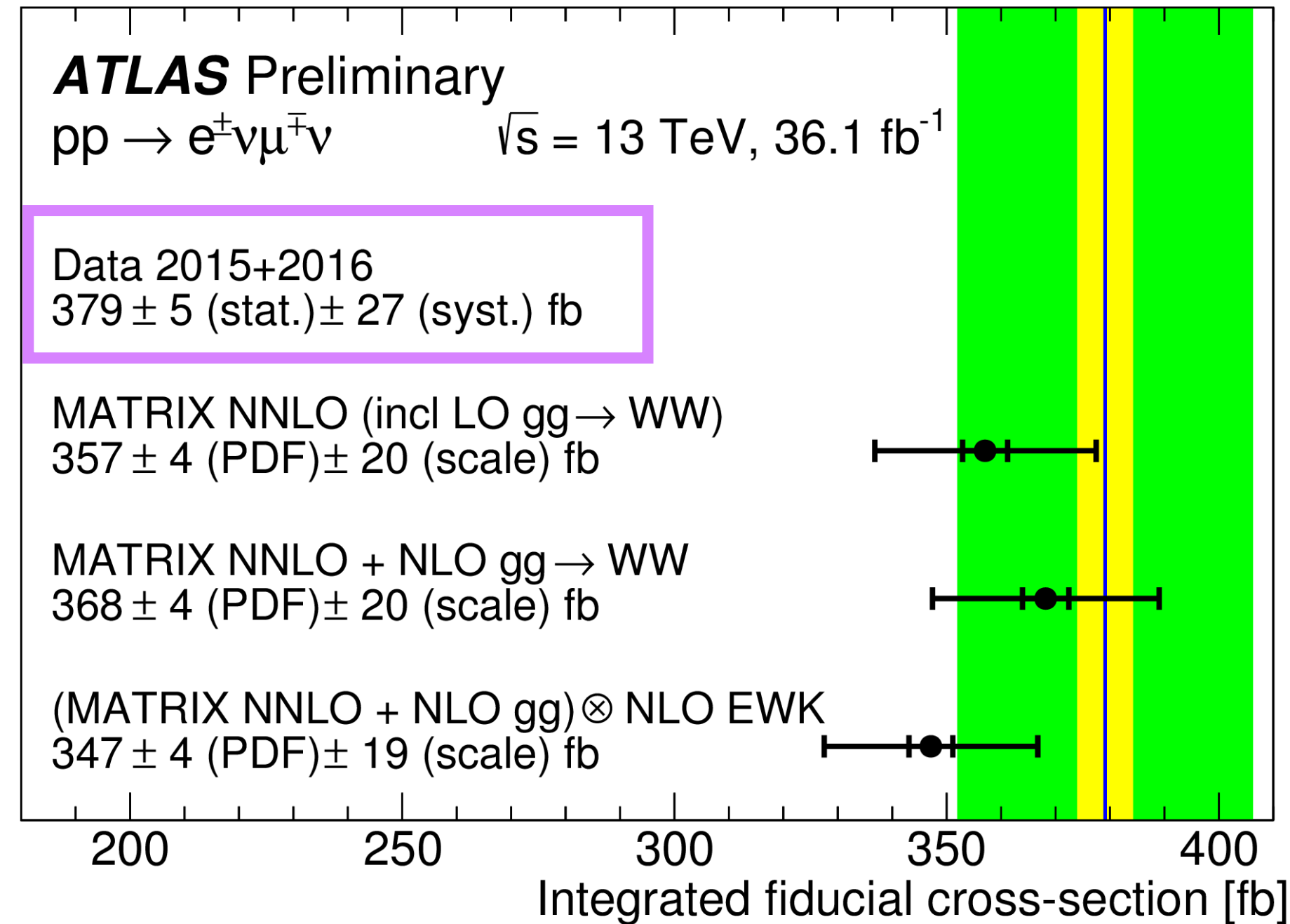
Fiducial Cross-Section:

- The measured and predicted fiducial cross-sections for the $W^+W^- \rightarrow e^\pm\nu\mu^\mp\nu$ signal process are shown here.

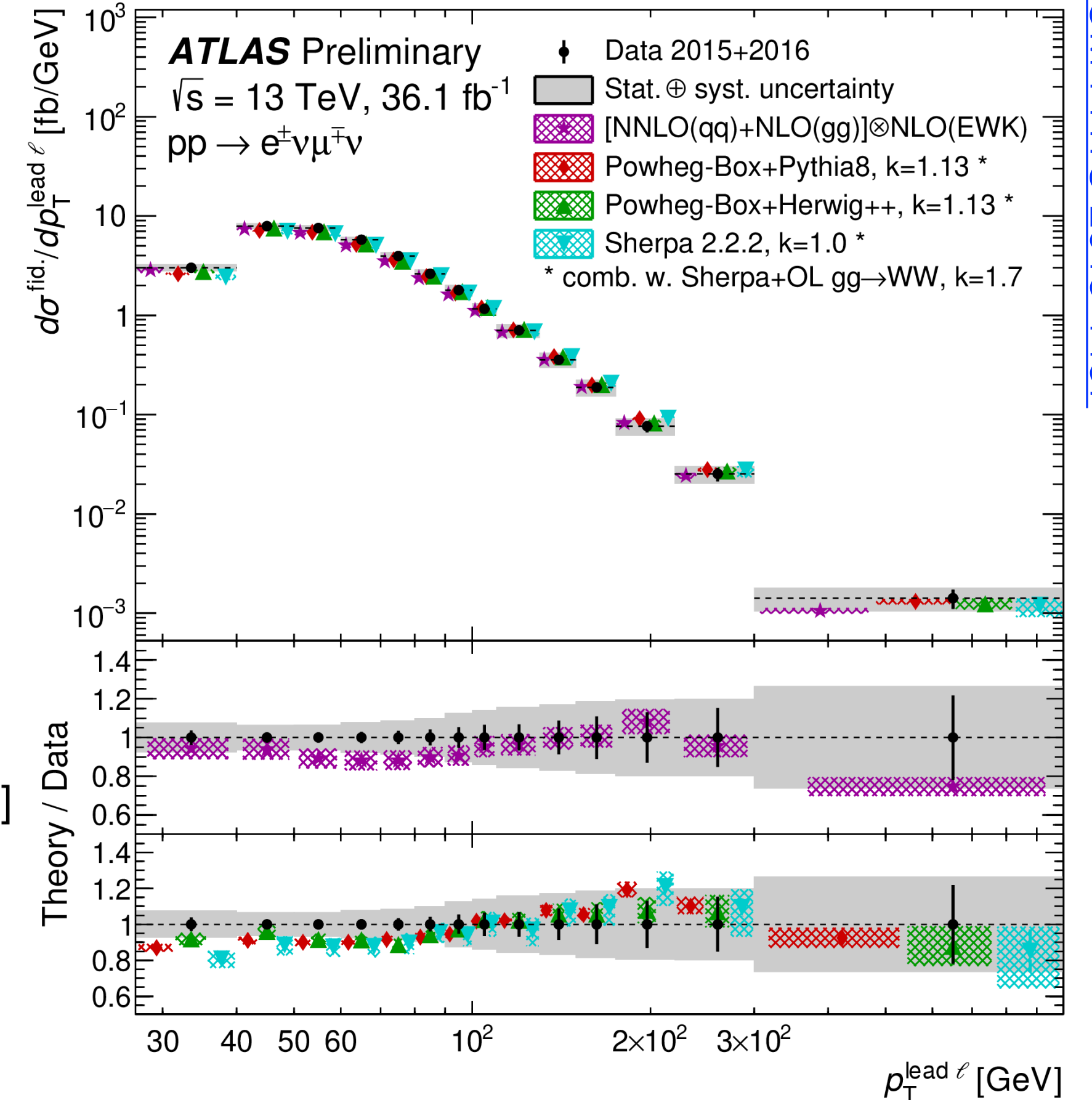
$$\sigma_{WW \rightarrow e\mu}^{\text{fid.}} = \frac{N_{\text{obs}} - N_{\text{bkg}}}{C \times \mathcal{L}}$$

- Good agreement exists between the measured and predicted fiducial cross-sections.

Comparison of the Measured and Predicted Fiducial Cross-Sections



Differential Cross-Section as a Function of Leading Lepton p_T



Differential Cross-Section:

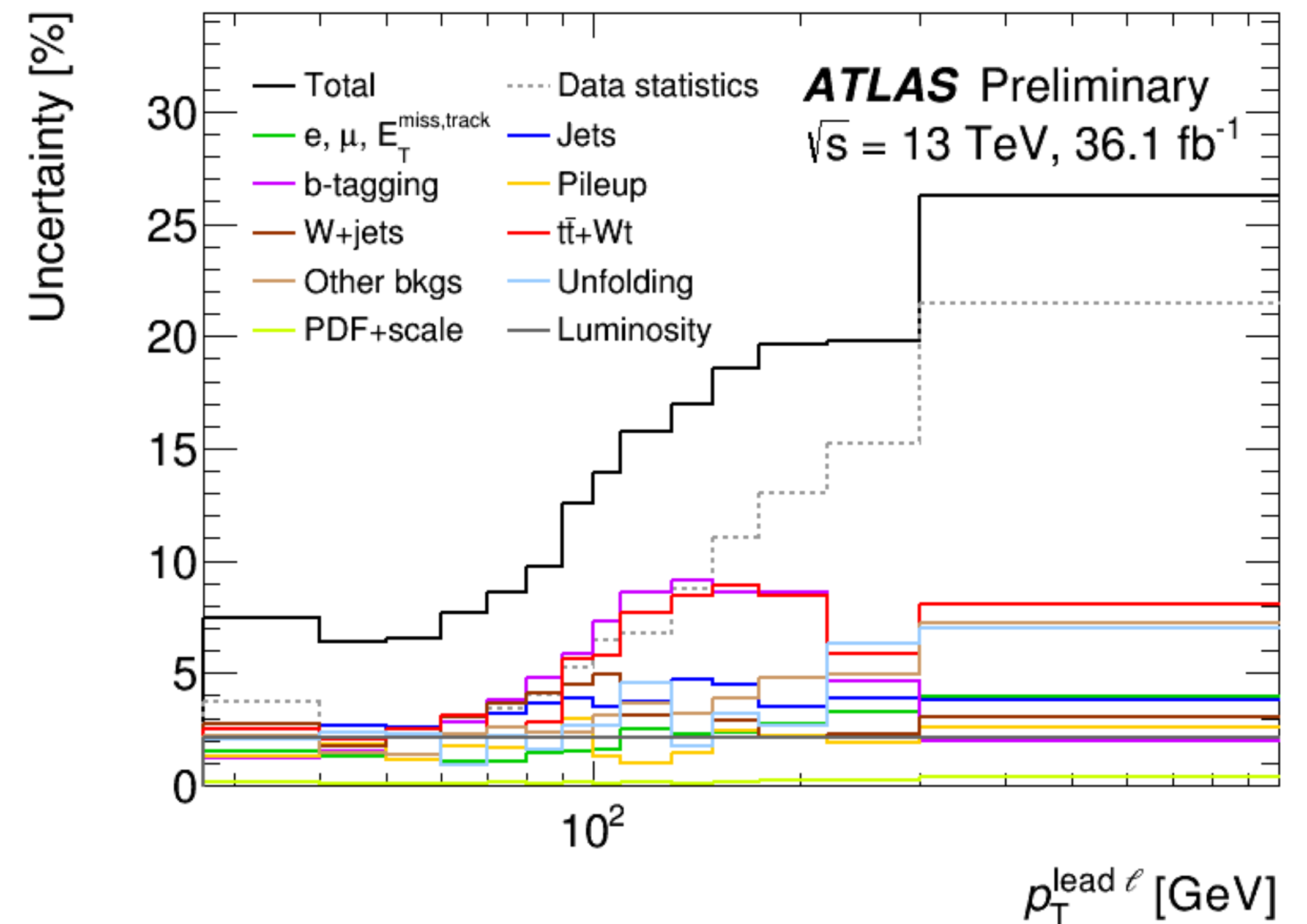
- An iterative Bayesian unfolding procedure is used to find the differential cross-section as a function of a number of lepton based observables.
- All of the predictions for each of the observables do a fair job of predicting the unfolded data. However, as seen here at low leading lepton p_T , there is a tendency to under predict the data.

- In the framework of effective field theory (EFT) there are five dimension six operators, \mathcal{O}_i , that can generate aTGCs from purely electroweak processes.

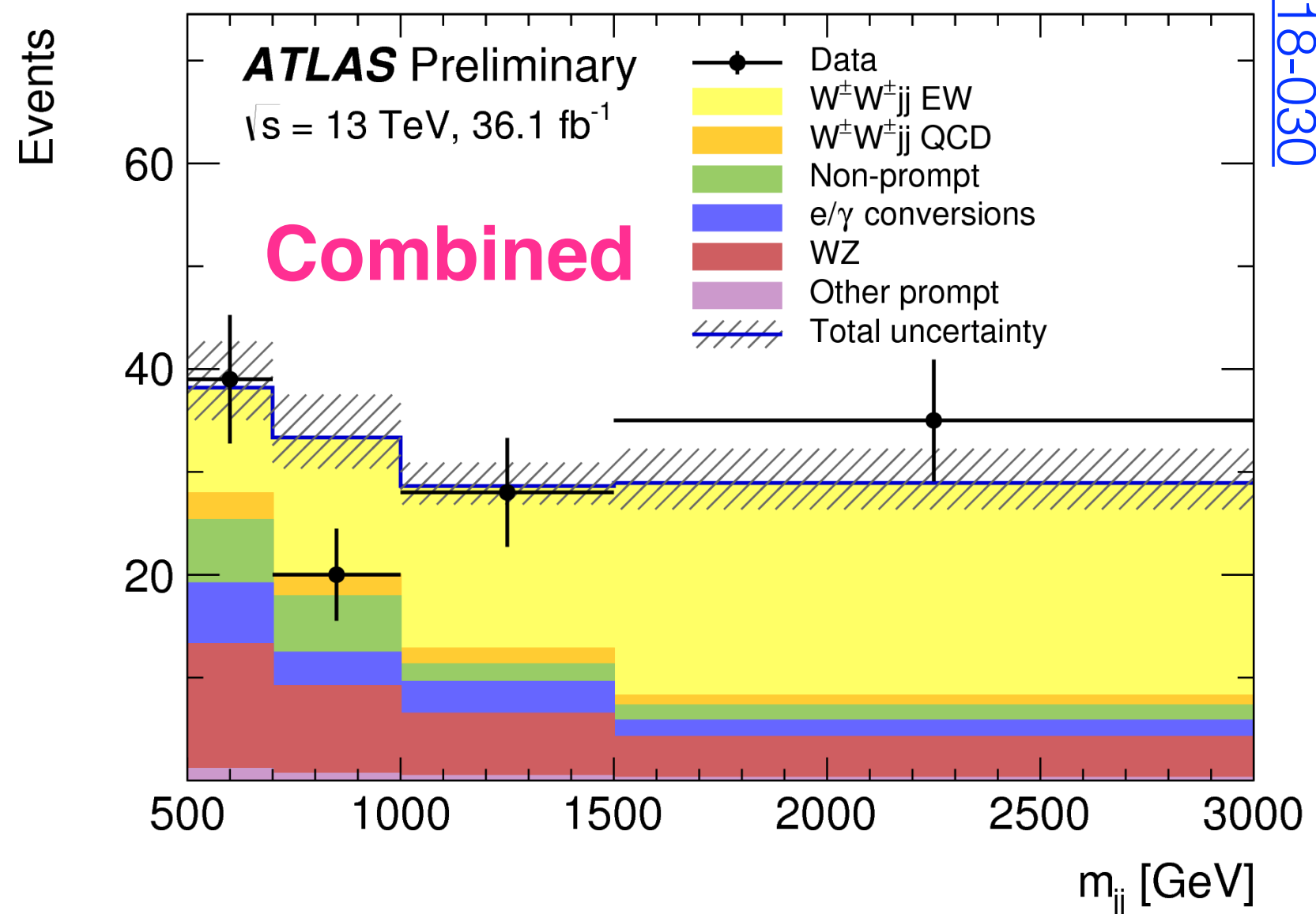
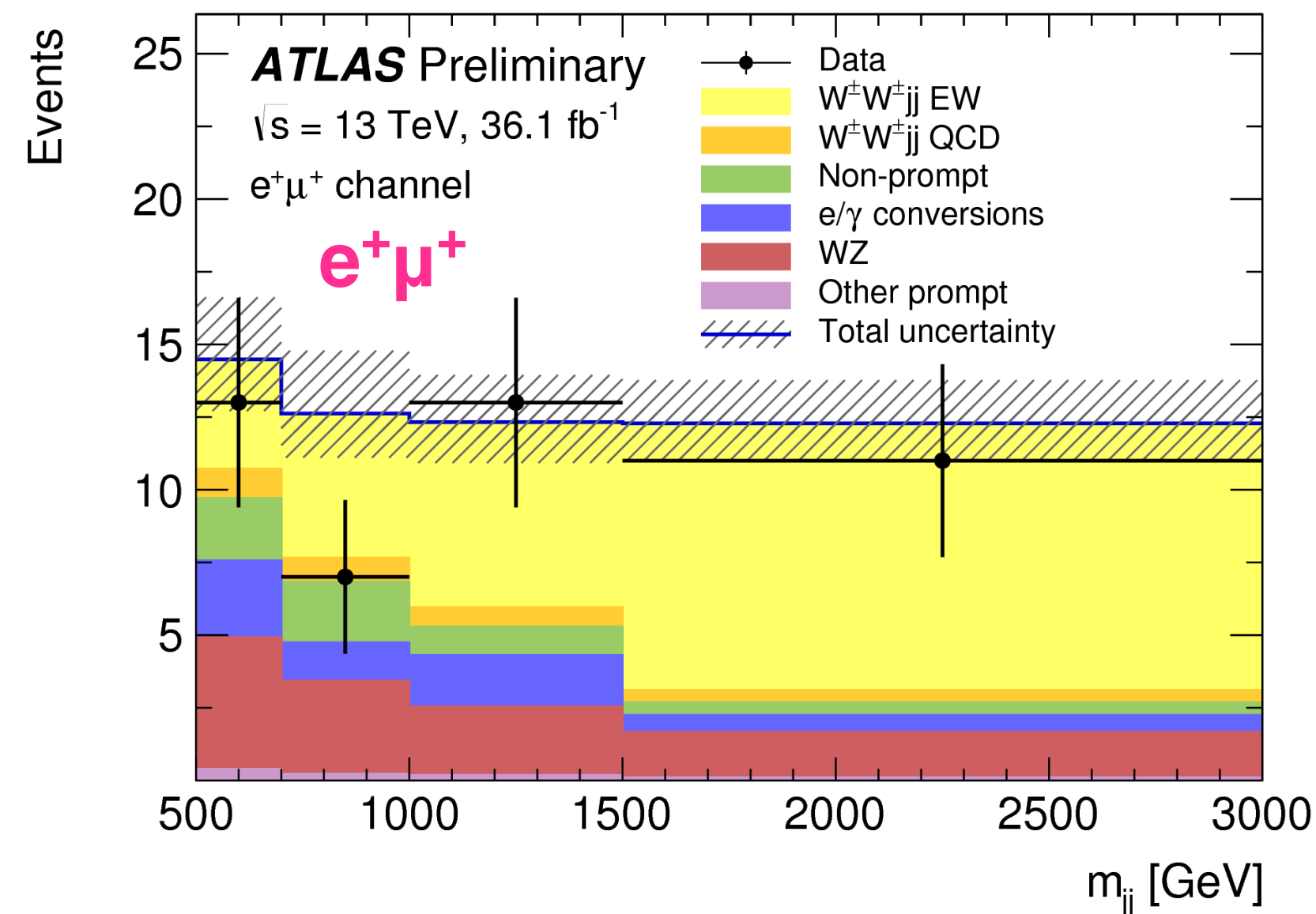
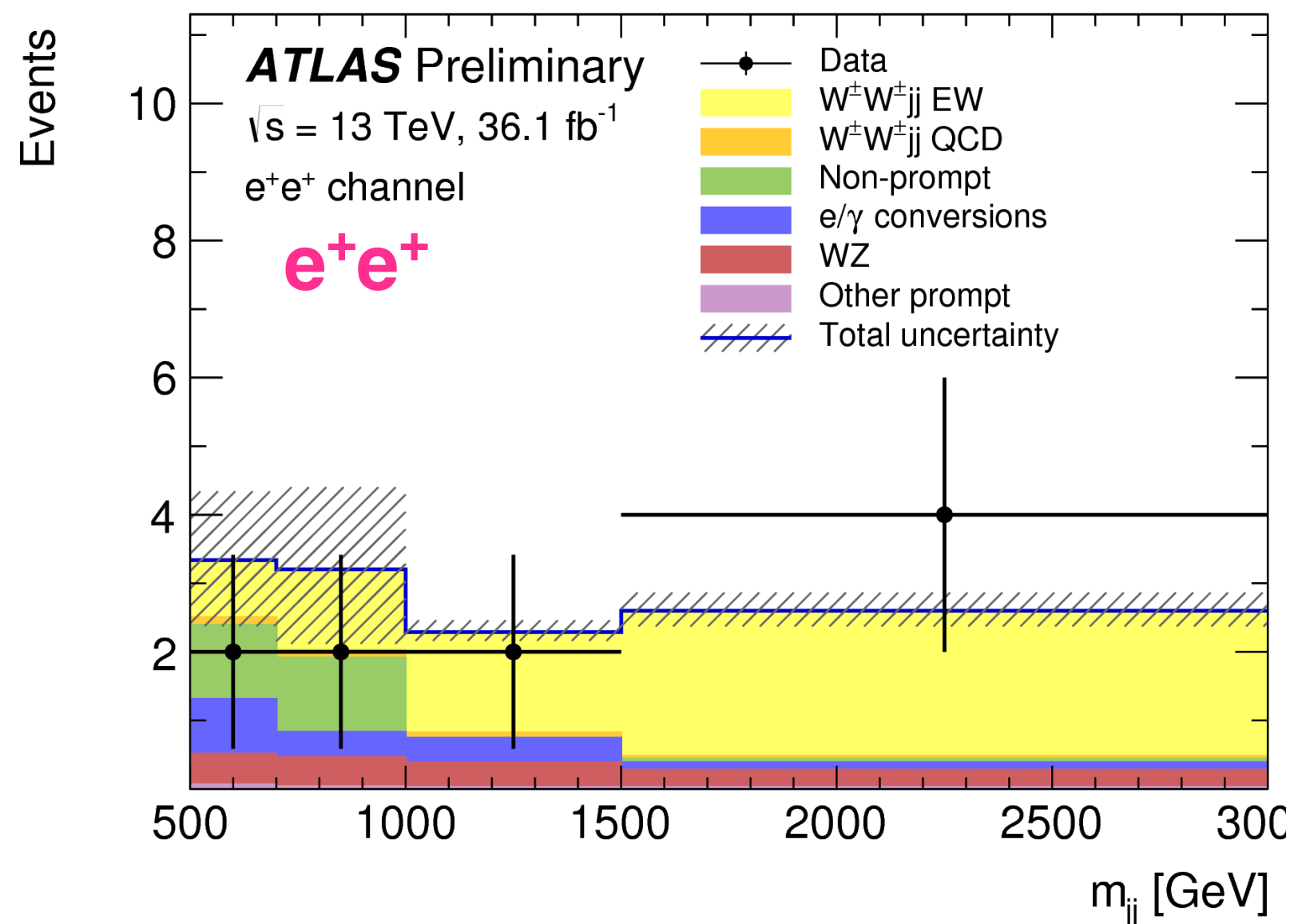
$$\mathcal{L} = \mathcal{L}_{\text{SM}} + \sum_i \frac{c_i}{\Lambda^2} \mathcal{O}_i$$

- Using the unfolded leading lepton p_T distribution it is possible to constrain the five associated EFT coefficients, c_i .
- The observed and expected 95% CL intervals for these coefficients are listed in the table.
- The plot to the right is a breakdown of the sources of uncertainty on the leading lepton p_T distribution.
- Sensitivity to anomalous couplings is greatest in the high leading lepton p_T bins.
- Since these bins are statistics dominated, further improvements to the constraints on the EFT coefficients will require a significant improvement in statistics.

Parameter	Observed 95% CL [TeV ⁻²]	Expected 95% CL [TeV ⁻²]
c_{WWW}/Λ^2	[-3.4, 3.3]	[-3.0, 3.0]
c_W/Λ^2	[-7.4, 4.1]	[-6.4, 5.1]
c_B/Λ^2	[-21, 18]	[-18, 17]
$c_{\tilde{W}WW}/\Lambda^2$	[-1.6, 1.6]	[-1.5, 1.5]
$c_{\tilde{W}}/\Lambda^2$	[-76, 76]	[-91, 91]



- For the VBS same-sign WW analysis, to increase sensitivity to the electroweak signal, events are grouped according to lepton decay channel, ($e^\pm e^\pm$, $\mu^\pm \mu^\pm$, and $e^\pm \mu^\pm$).
- Shown here are m_{jj} distributions for two of the six lepton decay channels. Also shown is the combined result.



- Shown here is a breakdown of the total number of expected signal and background events along with the number of observed data events for all lepton channels.
- Based on this, the electroweak $W^\pm W^\pm jj$ signal is observed and the background-only hypothesis is rejected with a significance of 6.9σ .

	Events
Expected Background	78 ± 15
$W^\pm W^\pm jj$ -EW	40.9 ± 2.9
Data	122

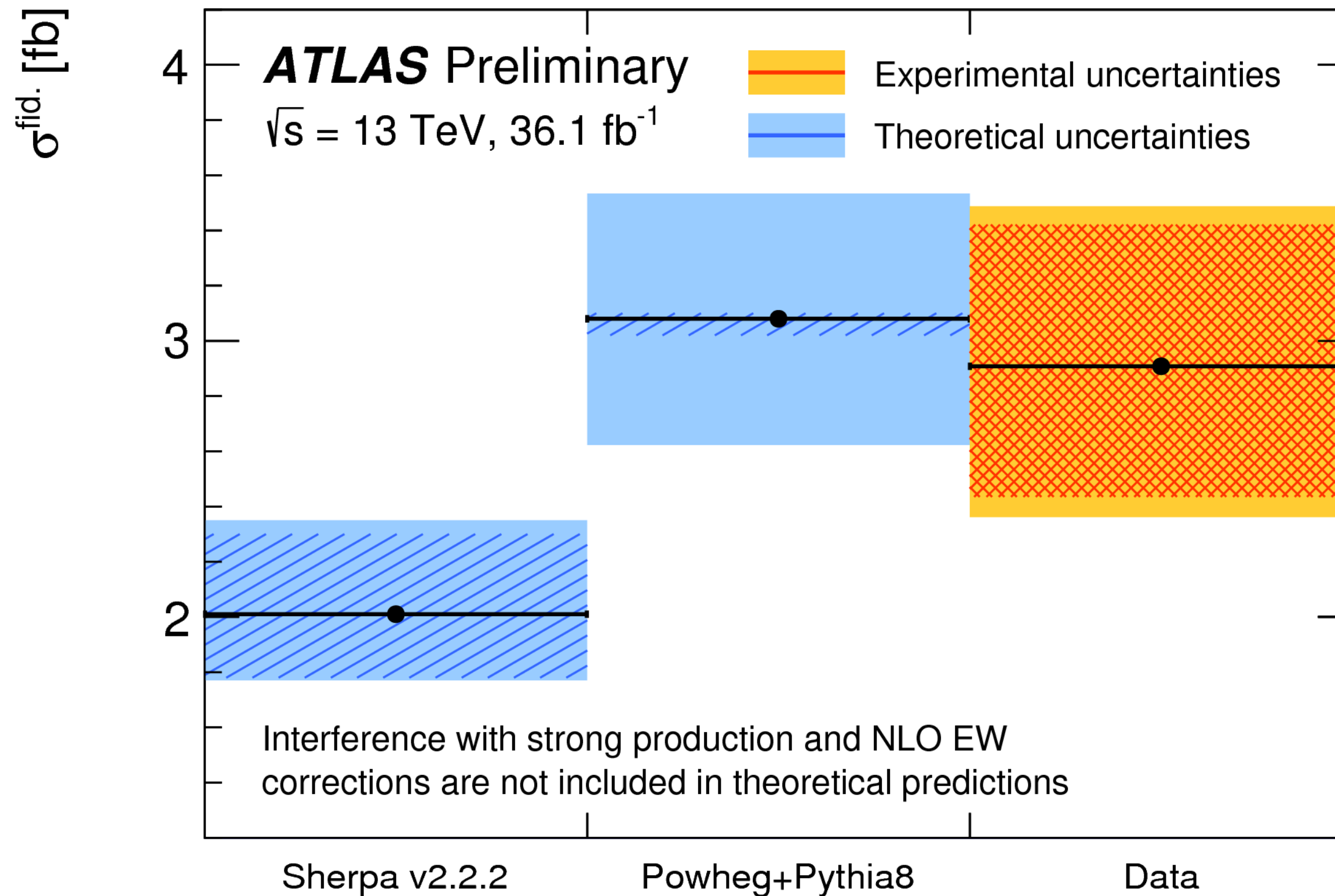
Fiducial Cross-Section:

- The fiducial cross-section is extracted from a profile likelihood fit of the m_{jj} distribution.
- Measured cross-section:

$$\sigma^{fid} = 2.91^{+0.51}_{-0.47} \text{ (stat.)} \pm 0.27 \text{ (syst.) fb}$$

- Shown to the right is a comparison of the observed and predicted values for the fiducial cross-section.
- The observed cross-section includes interference between the electroweak and strong production.
- The predictions do not include strong interference effects and they do not include NLO electroweak corrections.

Observed & Predicted Fiducial Cross-Section



- As part of its ongoing studies into the nature of the particles produced in high energy proton-proton collisions, the ATLAS detector has been used to perform the following set of recent measurements involving electroweak vector-boson pair production:
 - The fiducial and differential cross-sections for invisible Z production and limits on the parameters in the effective vertex function approach to describing aTGC contributions.
 - The differential cross-section as a function of the four-lepton invariant mass $m_{4\ell}$, the strength of gluon-induced 4ℓ production, the branching fraction of $Z \rightarrow 4\ell$, constraints on the off-shell Higgs boson signal strength and constraints on some modified Higgs boson couplings.
 - The fiducial and differential cross-sections of inclusive $W^\pm Z$ production and the longitudinal helicity fractions for W^\pm and Z bosons.
 - The fiducial and differential cross-sections of electroweak $W^\pm Zjj$ production.
 - The fiducial and differential cross-sections for leptonically decaying W^+W^- and constraints on the associated five EFT dimension six operators.
 - The fiducial cross-section for leptonically decaying VBS same-sign $W^\pm W^\pm$ production and a rejection of the background-only hypothesis.

- For an in-depth discussion of the analysis and results presented in this talk, please see the following:
 - The ATLAS Collaboration. Measurement of the $Z\gamma \rightarrow \nu\bar{\nu}\gamma$ production cross section in pp collisions at $\sqrt{s} = 13$ TeV with the ATLAS detector and limits on anomalous triple gauge-boson couplings. High Energy Phys. (2018) 2018: 10. [https://doi.org/10.1007/JHEP12\(2018\)010](https://doi.org/10.1007/JHEP12(2018)010).
 - The ATLAS Collaboration. Measurement of the four-lepton invariant mass spectrum in 13 TeV proton-proton collisions with the ATLAS detector. High Energy Phys. (2019) 2019: 48. [https://doi.org/10.1007/JHEP04\(2019\)048](https://doi.org/10.1007/JHEP04(2019)048).
 - The ATLAS Collaboration. Measurement of $W^\pm Z$ production cross sections and gauge boson polarisation in pp collisions at $\sqrt{s} = 13$ TeV with the ATLAS detector. eprint [arXiv:1902.05759 \[hep-ex\]](https://arxiv.org/abs/1902.05759).
 - The ATLAS Collaboration. Observation of electroweak $W^\pm Z$ boson pair production in association with two jets in pp collisions at $\sqrt{s} = 13$ TeV with the ATLAS detector. eprint [arXiv:1812.09740 \[hep-ex\]](https://arxiv.org/abs/1812.09740).
 - The ATLAS Collaboration. Measurement of fiducial and differential W^+W^- production cross sections at $\sqrt{s} = 13$ TeV with the ATLAS detector. CDS Record: [ATL-COM-PHYS-2018-1487](https://cds.cern.ch/record/1487).
 - The ATLAS Collaboration. Observation of electroweak production of a same-sign W boson pair in association with two jets in pp collisions at $\sqrt{s} = 13$ TeV with the ATLAS detector. CDS Record: [ATLAS-CONF-2018-030](https://cds.cern.ch/record/1487).

Backup